Real Structure and Residual Stresses of Ground Laser Cladded H13 Tool Steel

K. Trojan[1,*], J. Čapek[1], J. Čech[2], N. Ganev[1], V. Ocelík[3], K. Kolařík[1]

[1] *Department of Solid State Engineering, Faculty of Nuclear Sciences and Physical Engineering, Czech Technical University in Prague, Trojanova 13, 120 00 Prague, Czech Republic*

[2] *Department of Materials, Faculty of Nuclear Sciences and Physical Engineering, Czech Technical University in Prague, Trojanova 13, 120 00 Prague, Czech Republic*

[3] *Department of Applied Physics, Zernike Institute for Advanced Materials, Materials Science group, University of Groningen, Nijenborgh 4, 9747 AG, Groningen, The Netherlands*

[*] *karel.trojan@fjfi.cvut.cz*

Abstract: Since laser cladding does not achieve such accuracy, after cladding the material, it is always necessary to machine the surface to the required final shape. In this article, the real structure, the surface state of the residual stresses and the hardness of the ground surface are studied. The values of these parameters significantly affect the properties of the surface and thus the service life of the repaired part. Compressive residual stresses on the ground surface were observed, as well as a hardness difference of up to 300 HV.

Keywords: laser cladding; X-ray diffraction; AISI H13 tool steel; real structure; residual stresses.

1 Introduction

AISI H13 hot working tool steel is one of the most common die materials used in metal and casting industries. Dies suffer damage due to wear and thermo-dynamic stresses during their lifetime [1]. Therefore, various methods have been developed for their repair, which is cheaper than manufacturing new ones. A great benefit of laser cladding in this field is high productivity with minimal influence of surrounding material due to low heat input. However, when cladding multiple layers, the previous layers are thermally affected, which can significantly modify their microstructure, real structure, and hardness. For this reason, not only the cooling rate but also the temperature history during the cladding affects the resulting microstructure [2].

Since laser cladding achieves less accuracy than, for example, the selective laser melting (SLM) process, which uses a powder bed, after cladding the material, it is always necessary to machine the surface to the required final shape [3]. It is crucial to carefully determine, whether by machining the part into the desired shape, an area with poorer mechanical properties does not reach the surface. This would lead to lower service life and consequently unprofitability of the laser cladding. Such a study has not been described in the available literature; therefore, it is necessary to research the state of the real structure and other mechanical properties on the machined surface.

2 Experiment

Laser cladding was carried using an *IPG 3kW Yt:YAG* fibre laser. Laser power density of 90 J/mm^2 was applied to form clads in multilayers. A five-layer sample was formed from six and seven overlapping beads on the substrate made from AISI H11 tool steel. The surface of the clad was ground using an oscillating surface grinder, when 1.7 mm from the contact has been removed.

Surface macroscopic residual stresses on the ground surface were determined by X-ray diffraction. The values of residual stresses were calculated from lattice deformations determined on the basis of experimental dependencies of $2\theta(\sin^2\psi)$ assuming biaxial state of residual stress (θ is the diffraction angle, ψ the angle between the sample surface and the diffracting lattice planes). The diffraction angle was determined as the centre of gravity of the Cr$K\alpha_1\alpha_2$ doublet diffracted by the lattice planes $\{211\}$ of the α-Fe phase. The X-ray elastic constants ½s_2 = 5.76 TPa^{-1}, s_1 = –1.25 TPa^{-1} were used for the stress calculation. The experimental error is the standard deviation according to the "$\sin^2 \psi$" residual stress calculation algorithm.

In order to determine the real structure, diffraction patterns were obtained in classical Bragg–Brentano focusing configuration with cobalt X-ray tube. Quantitative analysis was evaluated using the Rietveld analysis in the MStruct software.

Hardness was measured by the instrumented indentation technique. Tests were carried out on MHT micro-hardness tester with diamond Vickers indenter. Indentation cycle consisted of loading to a maximum force of 9.81 N, holding at maximum load, and unloading for 30 s, 10 s, and 30 s, respectively. Data were evaluated by the Oliver-Pharr method.

3 Results

Figs. 1 and 2 describes the surface macroscopic residual stresses of the ground surface in the L direction, i.e. in the cladding and grinding direction, and in the T direction, i.e. perpendicular, respectively. The average error of the residual stress calculation is 26 MPa for both directions. The maps consist of 33 values in three rows with a spacing of 4 mm and the data were linearly interpolated.

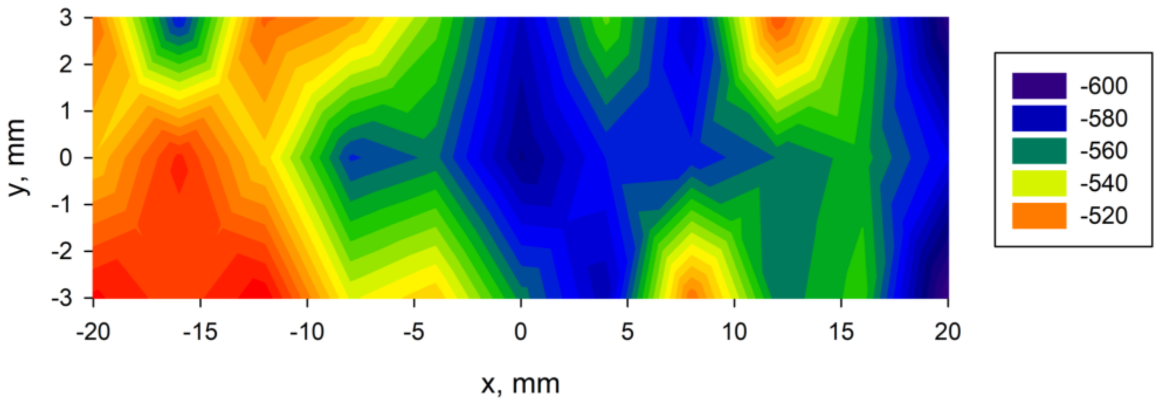

Fig. 1: Map of residual stresses [MPa] on the ground surface of the clad in the L direction.

From the point of view of the development of residual stresses during grinding, the direction of grinding is unfavourable, i.e. in the direction of the grinding lines (in this case the L direction). The material is strongly plastically deformed in this direction during grinding, which can cause tensile residual stresses, especially if the depth of cut per pass is large. However, only compressive residual stresses were detected in both directions. In the L direction, as expected, the compressive residual stresses reached smaller values (average value –551 MPa vs. –867 MPa in the T direction), but due to the small depth of cut per pass and sufficient cooling, tensile residual stresses did not occur.

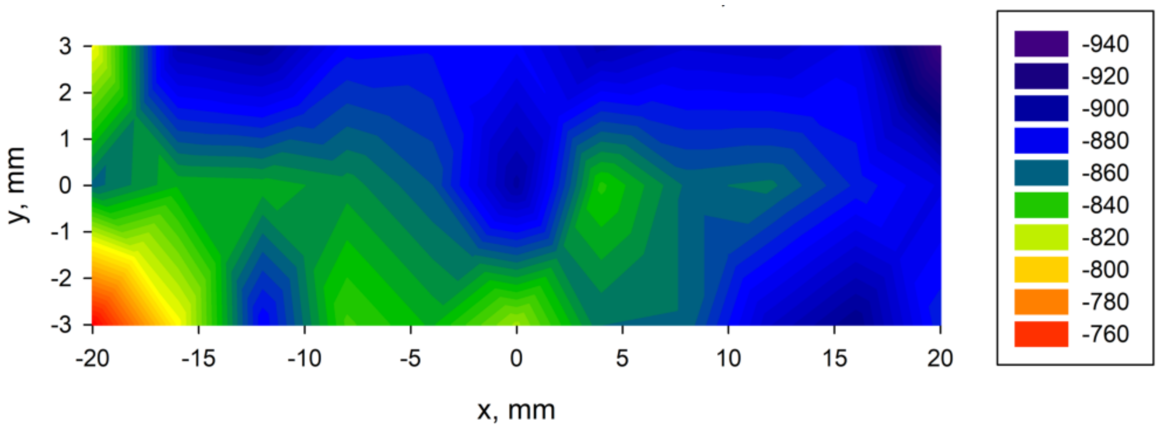

Fig. 2: Map of residual stresses [MPa] on the ground surface of the clad in the T direction.

From the figures describing the residual stresses of the ground surface, it can be seen that higher values of compressive stresses were found in the right part of the clad for both directions. This dependence was most likely caused by the cladding process, when the beads from which the clad was made end in the right part. Therefore, a different cooling rate and temperature history probably occurred in this area.

The real structure was determined by Rietveld refinement, where Fig. 3 denotes the crystallites size and Fig. 4 the microdeformation. The average crystallite size error is 0.8 nm and for microdeformations 1×10^{-4}. Slightly higher values of crystallite size were determined in the left half of the ground surface and, conversely, microdeformation was higher in the right. However, the obtained values show a low standard deviation – 1.2 nm and 1.8×10^{-4} which is almost comparable to the average error. Therefore, in terms of real structure the ground surface appears homogeneous.

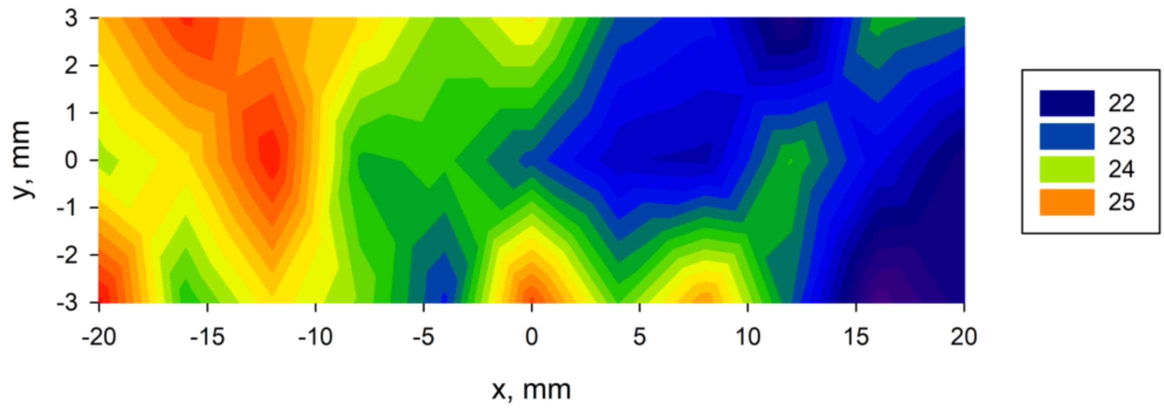

Fig. 3: Map of crystallite size [nm] of ferrite phase on the ground surface of the clad.

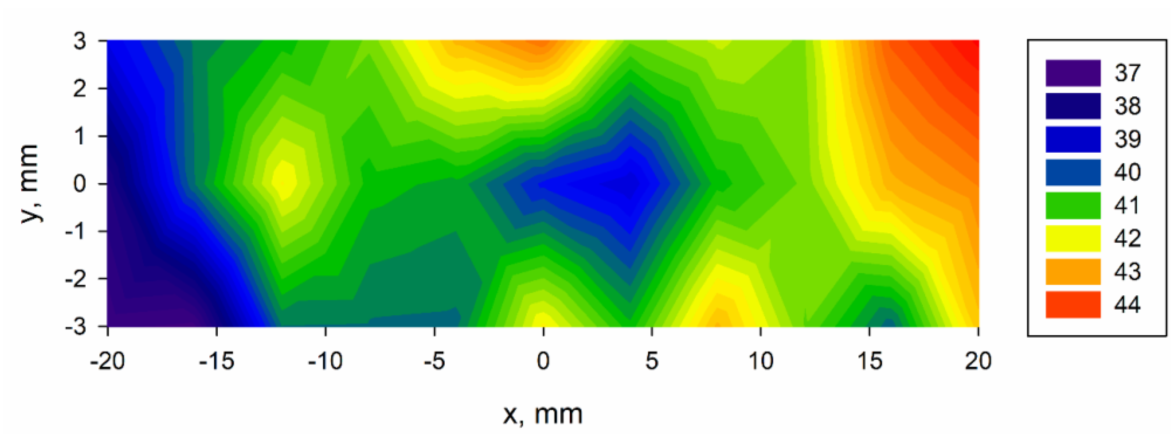

Fig. 4: Map of microdeformation [10^{-4}] of ferrite phase on the ground surface of the clad.

Fig. 5 defines the hardness $HV_{IT}1$ of the ground clad. The average hardness value is 681 $HV_{IT}1$ with a standard deviation of 50 $HV_{IT}1$. The map consists of 111 values in three rows and the data were linearly interpolated. At a distance of approx. x = –15 mm on the upper and lower side of the clad, the hardness reached only 535 $HV_{IT}1$. The occurrence of an area with a lower hardness value on the surface of the repaired part is unfavourable in terms of its service life.

It is also clear from the Fig. 5 that the higher hardness values are in the right part of the clad. Although the differences between microdeformation values and crystallite size are small, it is possible to observe that area with higher hardness values correlate with areas with smaller crystallite size and higher microdeformation. This is due to the concentration of dislocations and boundaries of crystallites, which in turn leads to higher hardness. In the area with higher hardness, the compressive residual stresses also reach higher values in both directions.

When optimizing the parameters of laser cladding, it would be appropriate from the point of view of service life to achieve the parameters that occur in the right part of the clad, where the beads always ended during the cladding process.

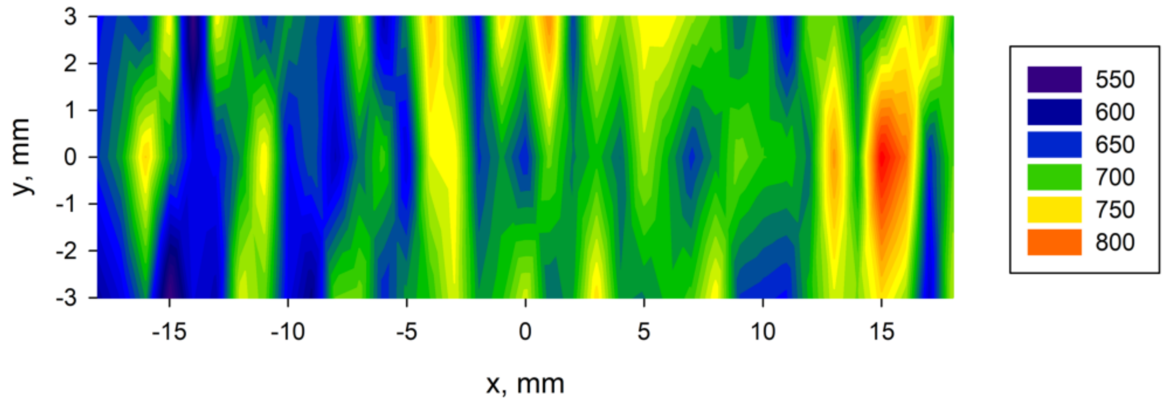

Fig. 5: Hardness [$HV_{IT}1$] map of the ground surface of the clad.

4 Conclusion

Laser deposition of the H13 tool steel showed great application potential. The ground surface showed compressive residual stresses in both directions, which are convenient from the point of view of component life. Even the real structure did not indicate large differences within the analysed ground surface. However, greater variance was observed at the hardness, when the difference between the highest value and the lowest was 300 HV. It is very important that areas with lower hardness did not cover a large part of the surface after machining. When optimizing the parameters of laser cladding, it would be appropriate from the point of view of service life to achieve the microstructure that occurs in the right part of the clad, where the beads always ended during the cladding process. This fact would be appropriate to investigate in further research using numerical methods.

Acknowledgement

Authors thanks to the project CZ.02.1.01/0.0/0.0/16_019/0000778 "Centre of advanced applied science" within the Operational Program Research, Development and Education supervised by the Ministry of Education, Youth and Sports of the Czech Republic. Laser cladding was performed at The University of Groningen, The Netherlands. K.T.'s work was supported by the Grant Agency of the Czech Technical University in Prague, grant No. SGS19/190/OHK4/3T/14.

References

[1] R.G. Telasang, et al., Microstructure and Mechanical Properties of Laser Clad and Post-cladding Tempered AISI H13 Tool Steel, Metall. Mater. Trans. A.46A (2015) 2309–2321, doi: 10.1007/s11661-015-2757-z.

[2] G. Roberts, et al., Tool Steels. Materials Park: A S M International, 1998.

[3] K. Salonitis, L. D'Alvise, B. Schoinochoritis. Additive manufacturing and post-processing simulation: laser cladding followed by high speed machining, Int. J. Adv. Manuf. Technol. 85 (2015) 2401–2411, doi: 10.1007/s00170-015-7989-y.